

Date of publication xxxx 00, 0000, date of current version xxxx 00, 0000.

Digital Object Identifier 10.1109/ACCESS.2022.Doi Number

Sub-6 GHz Band Omnidirectional Horizontally Polarized Large Spacing Array Antenna with Dielectric Radome for Base Station

Junyi Xu¹, Student Member, IEEE, Sirao Wu¹, Student Member, IEEE, and Qiang Chen¹, Senior Member, IEEE

¹Department of Communications Engineering, Graduate School of Engineering, Tohoku University, Sendai, Miyagi, 980-8579, Japan

Corresponding author: Junyi Xu (e-mail: xu.junyi.p8@dc.tohoku.ac.jp).

These research results were obtained from the commissioned research (No. 02201) by National Institute of Information and Communications Technology (NICT), Japan.

ABSTRACT A Sub-6 GHz band radome-covered omnidirectional horizontally polarized large spacing array antenna is reported with low grating lobe and low mutual coupling. A designed passive radome is utilized to replace several layers of active elements under the same effective aperture. The radome extends the current distribution and thus increases the effective aperture of the array element so that the array element spacing can be enlarged. Fewer antenna element is required with the radome introduced, compared with conventional spacing antenna array. Meanwhile, the large spacing decreases the mutual coupling between neighboring layers while no apparent grating lobe appears. The effectiveness of the proposed structure is evaluated by both simulation and experiment. And the mutual coupling and the grating lobe of proposed radome-covered antenna are also discussed. In the experiment, the 4-element 1-layer array model is considered. Proposed antenna is ideal for B5G application requiring fewer horizontal polarized sources covering the entire azimuth plane.

INDEX TERMS Large spacing array antennas, Fewer elements, Mutual coupling, Grating lobe, Dielectric radome

I. INTRODUCTION

As is known to all, omnidirectional antennas are attractive in wireless communication that require full coverage of the surrounding environment, such as cell phones [1-4], base stations [5-6], and WLAN [7], where an undirected circle radiation pattern on the horizontal plane is required. The two most basic implementations of the omnidirectional antenna are vertical polarization (VP) and horizontal polarization (HP). In typical indoor and urban environment, the vertically polarized omnidirectional antenna is always used [8-11]. As future communication systems require polarization diversity, the horizontally polarized (HP) [12-15] omnidirectional antenna is an essential complement.

Sub-6 GHz band is of importance in Beyond 5G (B5G) communication, due to its characteristics of low transmission loss, and low cost [16-17]. In Sub-6 GHz band, omnidirectional base stations can cover all the vehicles in a wide range, regardless of their location[18]. To realize the fast stable communication system, the collaboration

between antennas is often required in B5G base station deployments, which is called Centralized Radio Access Network(C-RAN) [19]. Only the radio units (RUs) or the antennas are set in the distributed base station, and all the signals are transmitted to centralized processing station for later calculation through optical fiber network. In this way, C-RAN has the advantage of facilitating control of interference suppression and improving area communication quality. It requires numerous distributed base station to cover the communication area [20]. However, the difficulty on practical application due to the infrastructure cost needs urgent solutions [21]. Under the premise of ensuring the directivity performance, the design of low-cost antenna by decreasing the number of antenna elements to reduce the complexity of antenna is one of the difficulties in fabricating modern base station antennas. In addition, due to the frequent occurrence of natural disasters recently, it is especially important to guarantee the emergency communication steady and continuously in the

harsh situation. Antennas that has simple structure and simple feeding network is much more reliable compared with large complex antenna arrays.

Over the past few decades, research on horizontally polarized omnidirectional antennas has proliferated as communication technologies have evolved. Most of them introduce antenna arrays to realize a base station antenna. In [5], a six-layer HP omnidirectional antenna array was proposed. Each layer required one power divider to feed the three elements in the layer, and feeding cables were needed for each layers. The feeding network is complex, which is a common phenomenon in conventional HP omnidirectional antenna array design. Also in [6], an eight-element linear antenna array was developed for 2G/3G base stations. Still eight layers of antenna element required eight coaxial cables as the feed source. Those antennas are not suitable for nowadays B5G antennas with simple structure and low cost needs.

Series-fed array antennas have only one feeding port which means simple structure. Many designs of series-fed antenna array were proposed such as franklin-like antenna array with phase inverters [22], uniform field distribution aperture structure [23], and MNG-TL loop antenna array [24]. The directivity of series-fed antennas has unavoidable upper limitation[25]. And the lengthened structure brings the side effect of high-order modes, so the structure of suppressing high-order modes increases the complexity of the feeder structure instead [23]. What's more, decreasing the number of antenna elements is another method to reduce the system complexity. Under the premise of the same effective aperture, the decrement of antenna elements in conventional antenna array leads to the increment of element spacing. It looks like a kind of sparse antenna array [26-27]. The large element spacing reduces the mutual coupling, which also provides the possibility of infrastructure-sharing [21]. In contrast, preventing grating lobe while keeping considerable directivity is the difficulty.

In this paper, a Sub-6 GHz band radome-covering omnidirectional horizontally polarized large spacing array antenna is reported for B5G application. Under the same effective aperture, a number of active elements are replaced by a specific passive radome. The radome increases the effective aperture of each array element by extending the current distribution, allowing for a larger array element spacing. The large spacing reduces mutual coupling between adjacent layers without creating significant grating lobes. Both simulation and experiment are used to evaluate the effectiveness of the proposed structure. The mutual coupling and the grating lobe of proposed radome-covering antenna are discussed. A 4-element 1-layer array model is considered in the experiment. Through the related literature search, it has not been found so far the same large spacing array antenna structure as the proposed radome-covered omnidirectional horizontal polarized array antenna.

The remaining sections of this article are organized as follows. Section II introduces the design of the fundamental large spacing antenna array, discusses its performance, and

explains its operating mechanisms. Section III presents the experiment on evaluating the effectiveness of the proposed large spacing array antenna. Finally, Section IV draws some conclusions and gives a detailed performance comparison between this work and other omnidirectional horizontally polarized array antennas.

II. THEORETICAL ANALYSIS AND ANTENNA DESIGN

To enhance the antenna directivity, a superstrate is introduced above a printed circuit antenna as a compact method [28]. Similarly, based upon this method, a cylindrical dielectric radome can be designed to enhance the performance of cylindrical antenna or antenna array. To evaluate the effect of the proposed antenna with radome, High-Frequency Structure Simulator (HFSS) from Ansys is utilized.

A. ANTENNA CONFIGURATION

The configuration of the proposed $M \times N$ elements base station antenna is shown in Fig. 1. The radius of the conducting cylinder is r_0 , which influences the roundness of the radiation pattern. The radius and the thickness of the dielectric radome cylinder are r_2 and t with the relative permittivity ϵ_r . In this research, FR4 ($\epsilon_r=4.4$) is selected as the material of the radome. The HP dipole antenna is utilized as the fundamental array element. The array antenna has N layers and M elements in each layer. All the antenna elements are placed averagely on the circumference with the radius of r_1 . And the layers are placed with the layer spacing of h_{array} .

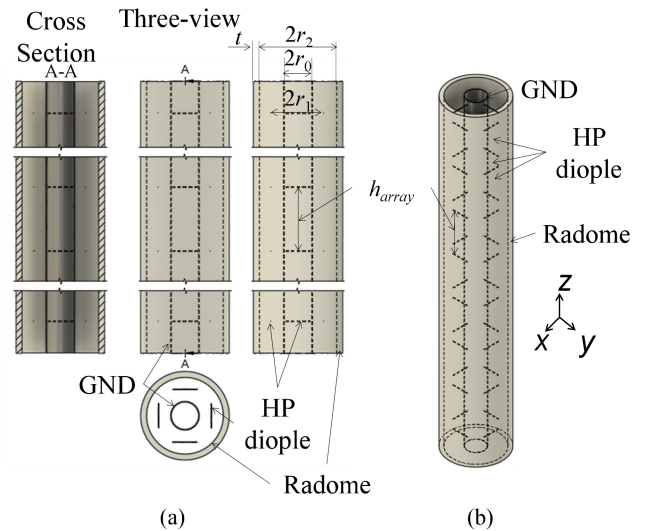


FIGURE 1. Proposed $M \times N$ elements array antenna with a radome surrounding. Taking 4-element 8-layer array as an example. (a) Three-view drawing and cross section. (b) Structure image.

B. OPERATING PRINCIPLE WITH SIMPLE STRUCTURE--FROM PLANE TO CYLINDER

For ease of understanding, Fig. 2 shows the structure of introducing only one element under the planar radome case and the cylindrical radome case. The radiation patterns

revealing the effectiveness of radome are presented in Fig. 3. It can be observed that for the planar case as shown in Fig. 3(a) the directivity increases by 7.4 dB. And for the cylindrical case as shown in Fig. 3(b) the directivity increment of 4.8 dB is smaller than planar case. It is because that in the cylindrical structure, the position relationship among the feed antenna, the cylindrical radome, and the cylindrical reflecting surface is not strictly parallel. Although the directivity enhancement is not as strong as that for the planar case, the performance improvement of the cylindrical antenna structure by the radome is still obviously effective.

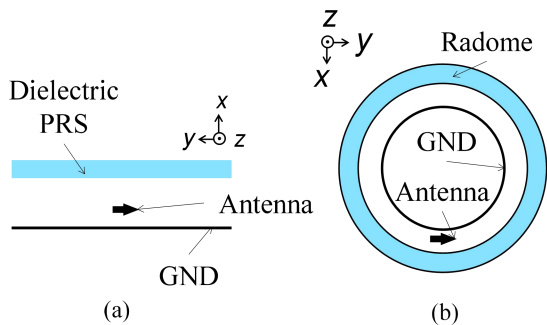


FIGURE 2. Simple structure of 1-element case proposed array antenna with radome covered. (a) Planar case. (b) Cylindrical case.

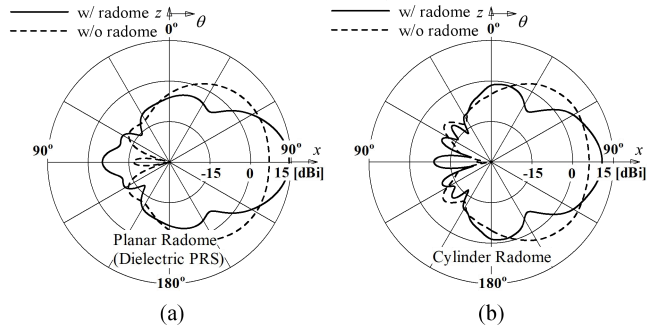


FIGURE 3. Radiation patterns of the antenna w/ and w/o radome in xoz plane. (a) Planar case. (b) Cylindrical case.

In Fig. 4, the electric field distributions along the observation line of a single element are plotted. It can be observed that the radome smooths and extends the effective current distribution and thus increases the effective aperture of the element, which gives the possibility to extend the distance between two adjacent elements when constructing an array. According to this, the radome-covered array antenna can establish a large spacing antenna array by fewer elements with more uniform field distributions on them. In this way, the proposed antenna can keep the directivity almost fixed with fewer elements under the same effective aperture.

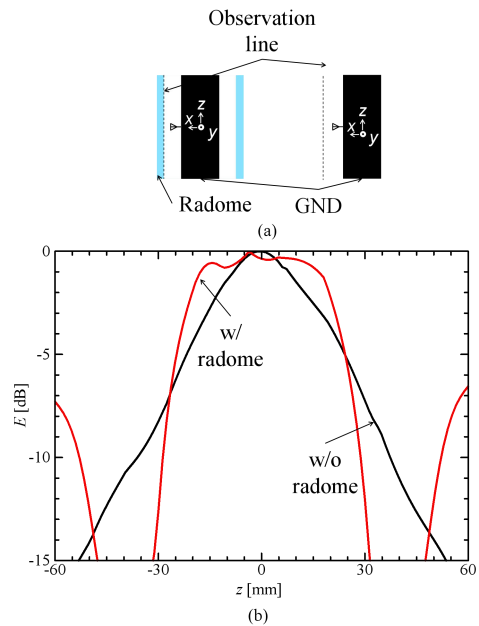


FIGURE 4. Comparison on electric field of antenna w/ and w/o radome (a) Electric field distribution along observation line. (b) Cross section of antenna w/ (red line) and w/o (black line) radome. (The dot line is the observation line.)

C. KEY DESIGN CONSIDERATION

There are several key aspects on designing the radome-covered large spacing antenna array, such as grating lobe and mutual coupling. The related parameters have led to general design guidelines of later omnidirectional large spacing antenna array design.

1) NO APPARENT GRATING LOBE

The radome-covered elements bring no apparent grating lobe even if the element spacing is over 1 wavelength, which is absolutely impossible in the conventional array antenna. Two elements are arranged with varied element spacing h_{array} to evaluate the grating lobe level just as shown in Fig. 5(a), and the normalized directivity on the vertical plane (xoz) is plotted in Fig. 5(b). With the introduction of the radome, no obvious grating lobe appears under the selected element spacing, even under 1.3 wavelength.

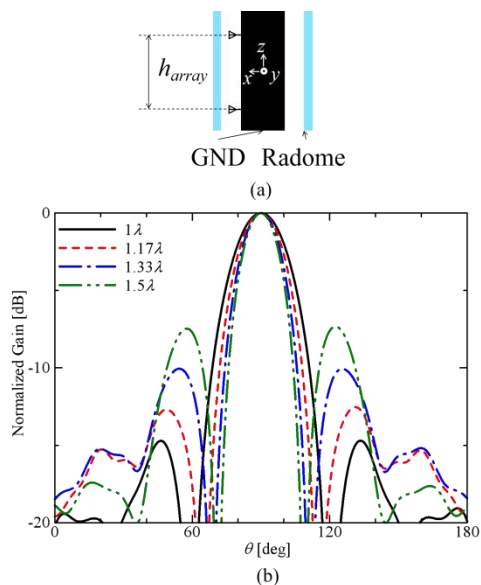


FIGURE 5. Evaluation on the grating lobe of antenna in 2-layer w/ radome case with the layer spacing of h_{array} . (a) Cross section. (b) Radiation patterns on vertical plane (xoz) with varied h_{array} .

2) LOW MUTUAL COUPLING

Because the element spacing is enlarged in this research, the mutual coupling between two neighboring elements is decreased. Fig. 6(a) shows the proposed 3-layer radome-covered large spacing array which is formed by removing the 2nd and 4th layers in the 5-layer conventional 0.5λ spacing no radome case. As shown in Fig. 6(b), around 15 dB decrement of the mutual coupling can be achieved near the operating frequency of 5 GHz.

D. OMNIDIRECTIONAL LARGE SPACING ANTENNA ARRAY--FROM DIRECTED TO UNDIRECTED

Based upon the discussion mentioned above, the proposed radome-covered structure can be used to design an omnidirectional horizontal polarized large spacing array antenna with fewer element layers. The basic antenna structure with the cylindrical radome discussed previously has only one element in each layer. For the omnidirectional radiation, an appropriate number of elements along circumferential direction are needed to meet the radiation pattern roundness requirement. In engineering application, the roundness of less than 3 dB is preferred [25,29]. Also, because the commonly defined directivity directivity is not suitable for evaluating omnidirectional antennas, the average directivity is used in this research. The definition of the average directivity is as followed.

$$D_a = \int_0^{2\pi} D_\phi d\phi / 2\pi \quad (1)$$

The roundness is influenced by the number of elements along the circumferential direction and the radius of the centered conducting cylinder. As shown in Fig. 7(a), the roundness for the 1-layer case with 3 elements does not meet the less than 3 dB requirement. Considering the fact that the thin conducting cylinder structure is difficult to fabricate, the

basic model of 4 elements in 1 layer is eventually used in this research.

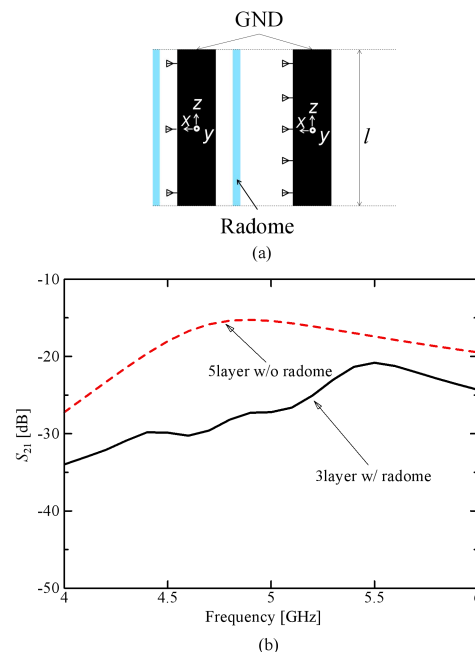


FIGURE 6. Comparison on mutual coupling of antenna in 3-layer w/ radome case and 5-layer w/o radome case. (a) Cross section. (b) Mutual coupling S_{21} .

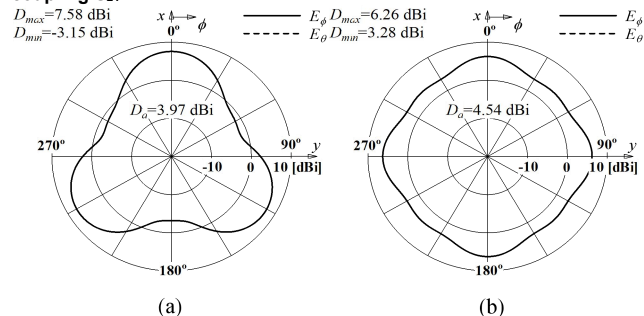


FIGURE 7. Radiation patterns of proposed 1-layer array antenna with a radome surrounding under varied elements. (a) 3-element case. (b) 4-element case.

1) FREQUENCY BANDWIDTH OF AVERAGE DIRECTIVITY UNDER ROUNDNESS REQUIREMENT AND THE EFFECTIVE APERTURE ENHANCEMENT OF ARRAY ELEMENT

A 1-layer 4-element model as shown in Fig. 8 is simulated. The parameters are set as $r_0=18$ mm, $r_1-r_0=15$ mm, and $r_2-r_1=15$ mm. The thickness of the radome t is $\lambda_g/4$, related to the material. The relationship between average directivity and frequency with varied materials is shown in Fig. 9. Only the average directivity that the roundness is less than 3 dB is plotted. CS-3396 material with relative permittivity of 10 is utilized to compare with FR4. It is obvious that high relative permittivity narrows the bandwidth of average directivity because the electrical thickness t/λ changes more significantly when the frequency varies.

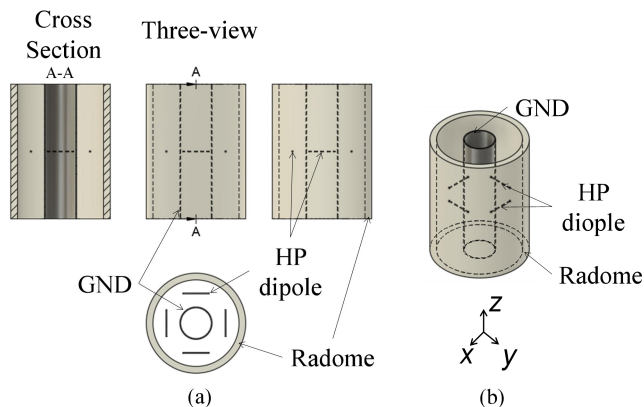


FIGURE 8. Proposed $M \times N$ elements array antenna with a radome surrounding. Taking 4-element 1-layer array as an example. (a) Three-view drawing and cross section. (b) Structure image.

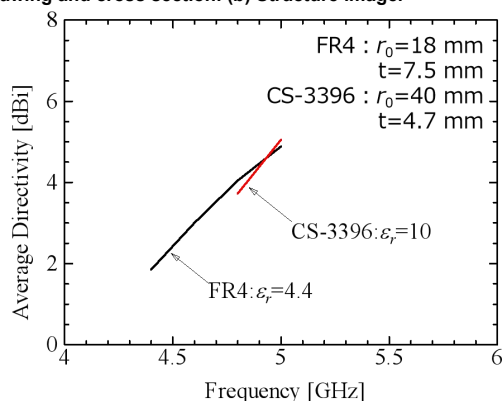


FIGURE 9. Average directivity and bandwidth under various radome material, where the bandwidth is the frequency bandwidth of average directivity when roundness is less than 3 dB. The thickness of the radome is $\lambda_g/4$ under each various permittivity.

The radiation patterns of the 1-layer 4-element antenna array are shown in Fig. 10. It can be seen from Fig. 10(a), without the radome, the roundness is 3.63 dB, which is not enough to meet the omnidirectional pattern requirement. Besides, although the maximum directivity in this case is 2.65 dBi, the average directivity is only 0.64 dBi. The result of radome-covered case is shown in Fig. 10(b). The maximum directivity is 6.26 dBi, which is significantly enlarged compared to the case without the radome. The average directivity also increases by 3.9 dB. At the same time, the roundness is reduced to 2.98 dB, showing good omnidirectional performance.

In our design, we use radome to compress the vertical plane radiation pattern so that the directivity on the horizontal plane can be improved. The radiation patterns of the 4-element antenna in the vertical plane (xoz) are shown in Fig. 11. The beamwidth of the antenna with radome is obviously narrower than that of the antenna without the radome. It means that more radiated energy is concentrated into the $\theta=90$ degree plane by introducing the dielectric radome.

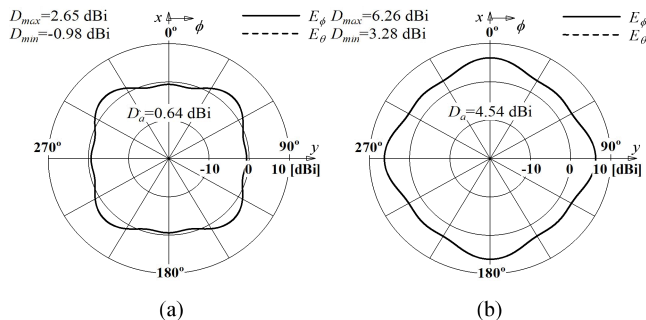


FIGURE 10. Radiation patterns of 4-element 1-layer array antenna on horizontal plane(xoy) with HP (a) Without radome. (b) With radome.

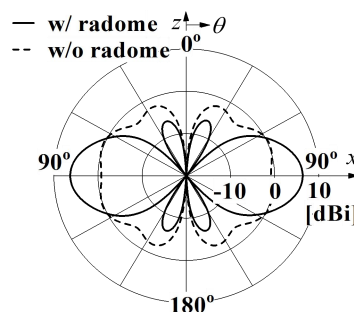


FIGURE 11. Radiation pattern of 4-element 1-layer array antenna on vertical plane(xoz) with horizontal polarization.

2) APPLICATION AND THE EVALUATION OF THE KEY DESIGN CONSIDERATIONS.

To acquire much higher directivity, the single-layer 4-element omnidirectional array can be used as a whole to implement a multi-layer antenna array. The configuration of the design is shown in Fig. 12(c). Under the same directivity, proposed 3-layer radome-covered large spacing array antenna is formed by removing the 2nd and 4th layers in the 5-layer conventional 0.5λ spacing no radome case. The layer spacing reaches one wavelength. As observed from Fig. 12(a), the average directivities of 7.5 dB are basically the same for both cases. The omnidirectional radiation pattern is still kept. Also, Fig. 12(b) shows that the grating lobe does not appear apparently. In contrast, as observed from Fig. 13, the grating lobe can not be ignored in the 1λ spacing array antenna without the radome. Under the same directivity level without undesired grating lobe, two layers of active elements can be replaced by the passive radome. The large spacing also leads to the decrement of mutual coupling between adjacent layers, as shown in Fig. 14. As proved in previous researches[30-33], enlarging the layer spacing is an effective method to decrease the mutual coupling between adjacent layers. Also, as the spacing in proposed antenna can be over 1 wavelength without apparent grating lobe, the mutual coupling is further decreased compared with conventional 0.7-0.8 wavelength case. Moreover, because the same directivity is guaranteed, fewer layers of antenna are used. Therefore the feeding network turns to be simple and the power cost is reduced.

For further high directivity gain, the number of layers is change to eight. As shown in Fig. 15, the average directivity increases by around 8 dB with the good roundness. Also, the beamwidth on the vertical plane is apparently narrowed, which leads to the directivity enhancement on the horizontal plane.

In summary, the proposed antenna utilizes the passive radome instead of a few layers of active elements. The radome enlarges the effective aperture of each layer so that fewer layer is required to realize a large spacing antenna array with fixed directivity. And the power cost of the proposed antenna is reduced, and the structure of the feeding system is simplified. The mutual coupling decreases due to the large layer spacing while no apparent grating lobes appears.

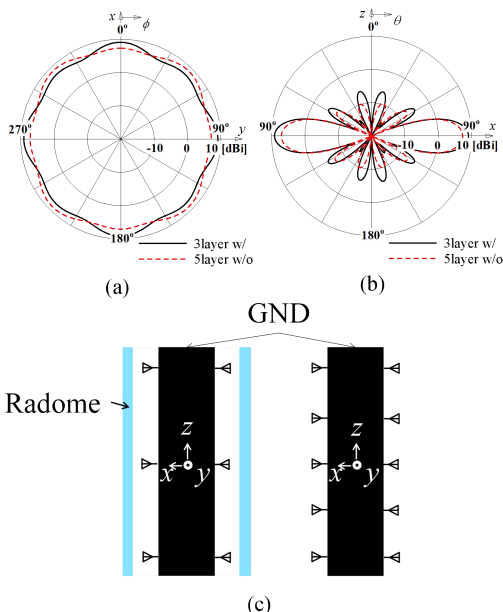


FIGURE 12. Radiation patterns with the same aperture of 3-layer w/ radome and 5-layer w/o radome. (a) Horizontal plane (xoy). (b) Vertical plane (xoz). (c) Simulation model of 3-layer w/ radome (left) and 5-layer w/o radome (right).

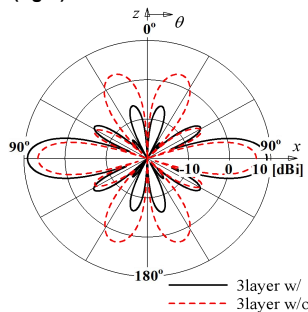


FIGURE 13. Radiation pattern of 4-element 3-layer w/ and w/o radome with $h_{array}=60$ mm on the vertical plane (xoz).

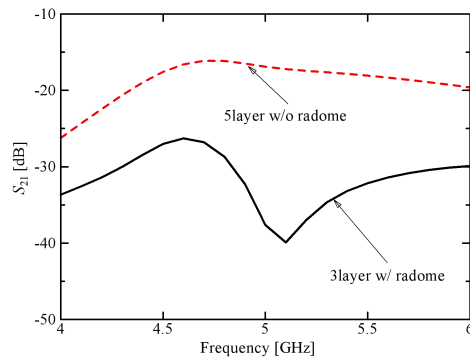


FIGURE 14. Mutual coupling between two neighboring omnidirectional layers in 3-layer w/ radome case and 5-layer w/o radome case.

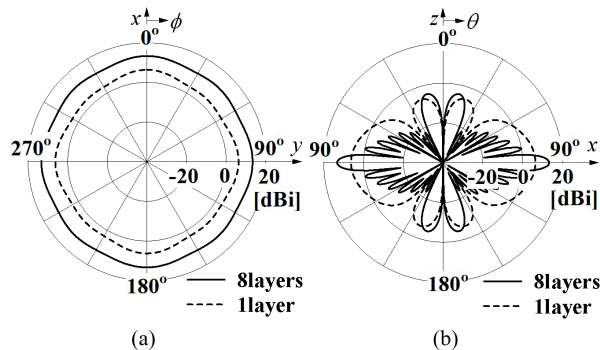


FIGURE 15. Radiation pattern of 1-layer and 8-layer radome-covered antenna. (a) Horizontal plane (xoy). (b) Vertical plane (xoz).

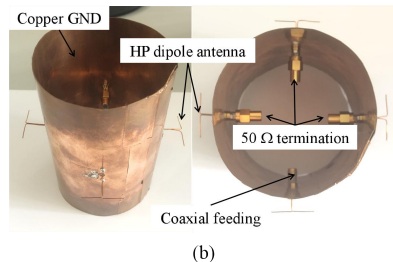
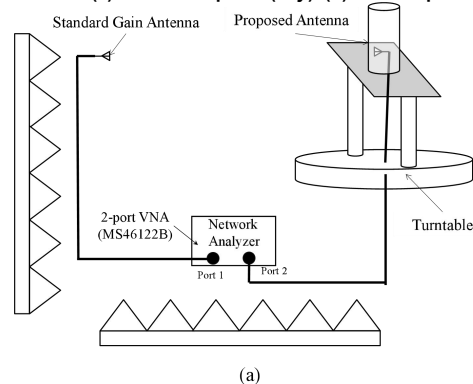


FIGURE 16. Experiment setup. (a) In the electromagnetic anechoic chamber. (b) Fabricated 4-element antenna under test.

III. MEASUREMENT RESULT

Fig. 16(a) shows the experimental setup to evaluate the proposed antenna consisting of the horizontal polarization dipole elements by the 2-port VNA (Anritsu MS46122B). The standard horn antenna is utilized as the receiving

antenna, and the proposed antenna as the transmitting one is placed on the turntable. To decrease the cable loss, the VNA is placed inside the electromagnetic anechoic chamber covered with absorbent material. And Fig. 16(b) shows the fabricated 1-layer 4-element horizontal dipole antenna array. To decrease the edge effect, a longer conductor cylinder with the length of $2\lambda=120$ mm is used. Due to the measurement environment, only 1 element is fed in the experiment, the other 3 elements are connected to the 50Ω impedance termination through the SMA connectors. The radiation pattern when 4 elements are fed can be observed from the composition of the single-fed radiation pattern by the superposition principle of the EM fields.

In the experiment, the CS-3396 with relative relative permittivity of 10 is selected as the material of the radome. The impedance changes more significantly compared with the case using FR4 in simulation. Fig. 17 shows that the matching condition in utilizing FR4 only slightly changes after introducing the radome, while it differs when using CS-3396. Therefore, in the experiment, the reflection losses are compensated mathematically in the measurement results. Still, in the engineering application, a matching network or some minor improvement on antenna element design is necessary to deal with the mismatching loss.

The radiation pattern in the horizontal plane (xoy) is shown in Fig. 18. The directivity is enlarged by around 4.11 dB using the dielectric radome, compared with the case without the radome. The vertical plane radiation pattern (xoz) is shown in Fig. 19, which shows a significant beamwidth decrease on this plane. It meets well with the phenomenon observed in simulation.

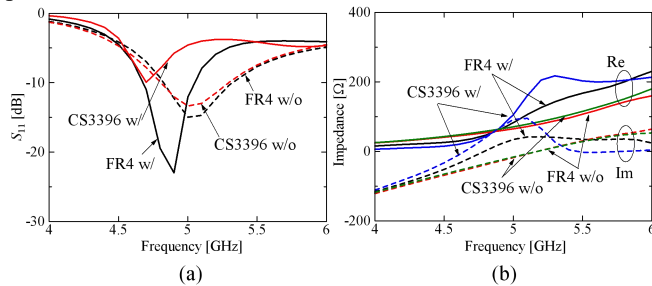


FIGURE 17. Influence to proposed antenna with radome made of different medium. (a) Reflection coefficient. (b) Impedance.

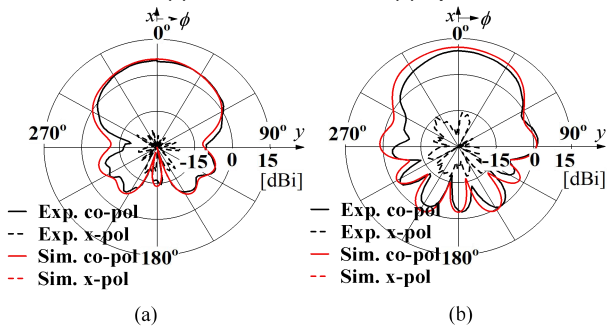


FIGURE 18. Experiment results and simulation results of radiation pattern feeding 1 element in all the 4-element on horizontal plane (xoy). (a) Without radome (b) With radome.

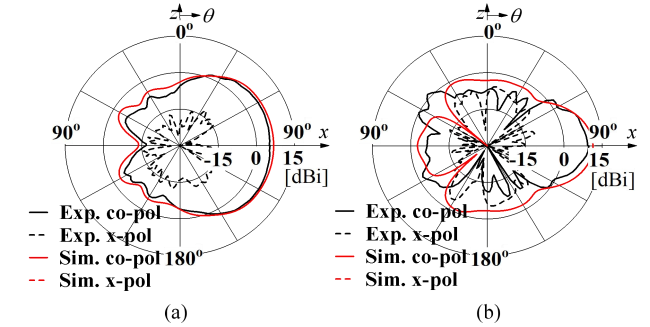


FIGURE 19. Experiment result and simulation results of radiation pattern feeding 1-element in all the 4-element on vertical plane (xoz). (a) Without radome (b) With radome.

Based on the EM field superposition principle, the radiation pattern of the antenna with all four elements fed is obtained. In Fig. 20, an obvious roundness decrement of 10.38 dB after the radome is introduced, although the 3.09 dB roundness is still slightly higher than the expected 3 dB. This can be improved by rotating the adjacent layer with the same frequency [5, 34-35] which is reported as a wideband solution for roundness. Also the average directivity is 2.67 dBi, which increases by 2.24 dB compared with the case without the radome. As shown in Fig. 21, the radiation pattern of 3-layer with radome case presented in Fig. 12 is calculated from the experiment result. The average directivity of calculation result is 7.44 dBi, which is similar with the simulation value of 7.5 dBi. It supports the correctness of the experiment. Also, as the array is the extension of 1-layer antenna with radome, 1-layer case can somewhat corroborate our proposed effect of radome. As the effective aperture of single layer is enlarged by the radome, fewer layer is required in realizing a large spacing antenna array with fixed physical aperture.

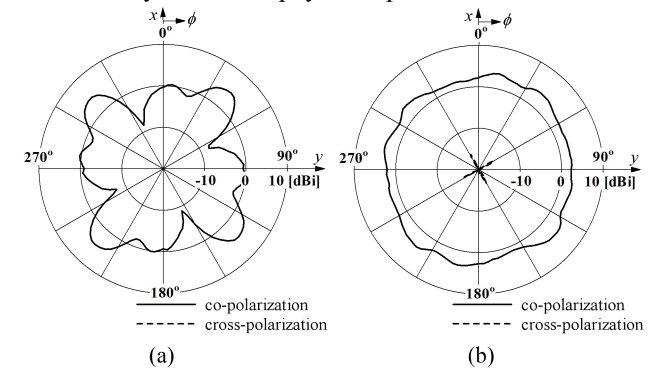


FIGURE 20. Calculation result of radiation pattern 4-element 1-layer array antenna on horizontal plane (xoy). (a) Without radome (b) With radome.

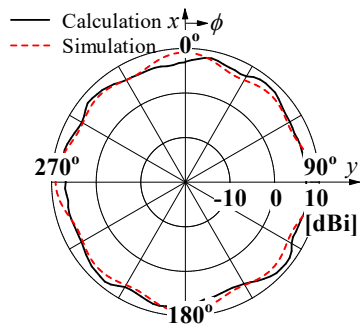


FIGURE 21. Radiation pattern of calculated 3-layer array case with radome covered comparing with the simulation result.

IV. CONCLUSION

A Sub-6 GHz band radome-covered omnidirectional horizontally polarized large spacing array antenna was reported for Beyond 5G (B5G) application. Under the same physical aperture, a number of active elements were replaced by a specific passive radome. The radome increased the effective aperture of each layer by extending the current distribution, allowing for a larger array element spacing and few layers. While no obvious grating lobe was apparent, the large spacing reduced the mutual coupling between adjoining layers. Both simulation and experiment were used to evaluate the effectiveness of the proposed structure. And the mutual coupling and the grating lobe of proposed radome-covered antenna were also in good performance.

TABLE I

HP OMNIDIRECTIONAL ARRAY ANTENNA DESIGN COMPARISON

Ref	Layers	Freq [GHz]	Directivity y [dBi]	Length [λ_0]	Directivity per unit length(dBi/ λ)
[7] 2019	6	1.67-2.73	PD ^a :9	3.5	PD:2.57
[9] 2020	8	9.6-10.4	PD:10.4	4.3	PD:2.42
[10] 2022	4	5.46-6.13	PD:10	4.62	PD:2.16
This work	3	5	AD ^b : 7.55(Sim.) PD: 9(Sim.)	3	AD: 2.52(Sim.) PD: 3(Sim.)

^aPD=Peak directivity, ^bAD=Average directivity.

To better address the advantages of the proposed design, comparisons with other HP omnidirectional antennas are tabulated in Table I. Among all the listed antennas, our proposed design can achieve the highest directivity per unit length. Besides, our work reaches the same directivity with the fewest layers, which means the low power cost and simple feeding network. What’s more, the large layer spacing does not bring the grating lobe while the mutual coupling between neighbored layers is decreased.

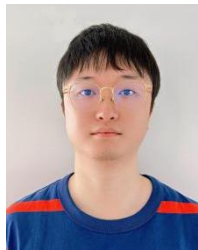
ACKNOWLEDGMENT

These research results were obtained from the commissioned research (No. 02201) by National Institute of Information and Communications Technology (NICT), Japan.

REFERENCES

- [1] K. Fan, Z. -C. Hao, Q. Yuan, J. Hu, G. Q. Luo and W. Hong, "Wideband Horizontally Polarized Omnidirectional Antenna With a Conical Beam for Millimeter-Wave application," *IEEE Trans. Antennas Propag.*, vol. 66, no. 9, pp. 4437-4448, Sept. 2018.
- [2] C. Zhang, X. Liang, X. Bai, J. Geng and R. Jin, "An UHF Tree-Like Biconical Antenna With Both Conical and Horizontal Omnidirectional Radiations," *IEEE Antennas Wireless Propag. Lett.*, vol. 14, pp. 187-189, 2015.
- [3] Z. D. Wang, Y. Z. Yin, X. Yang and J. J. Wu, "Design of a Wideband Horizontally Polarized Omnidirectional Antenna With Mutual Coupling Method," *IEEE Trans. Antennas Propag.*, vol. 63, no. 7, pp. 3311-3316, July 2015.
- [4] H. -Y. Zhang, F. -S. Zhang, F. Zhang, T. Li and C. Li, "Bandwidth Enhancement of a Horizontally Polarized Omnidirectional Antenna by Adding Parasitic Strips," *IEEE Antennas Wireless Propag. Lett.*, vol. 16, pp. 880-883, 2017.
- [5] L. H. Ye, Y. Zhang, X. Y. Zhang and Q. Xue, "Broadband Horizontally Polarized Omnidirectional Antenna Array for Base-Station application," *IEEE Trans. Antennas Propag.*, vol. 67, no. 4, pp. 2792-2797, April 2019.
- [6] Quan, Xu Lin, et al. "Development of a broadband horizontally polarized omnidirectional planar antenna and its array for base stations." *Prog. Electromagn. Res.*, 128 (2012): 441-456.
- [7] J. Guo, H. Bai, A. Feng, Y. Liu, Y. Huang and X. Zhang, "A Compact Dual-Band Slot Antenna With Horizontally Polarized Omnidirectional Radiation," *IEEE Antennas Wireless Propag. Lett.*, vol. 20, no. 7, pp. 1234-1238, July 2021.
- [8] K.-L. Wong, F.-R. Hsiao, and T.-W. Chiou, "Omnidirectional planar dipole array antenna," *IEEE Trans. Antennas Propag.*, vol. 52, no. 2, pp. 624-628, Feb. 2004.
- [9] K. Wei, Z. Zhang, W. Chen, Z. Feng, and M. F. Iskander, "A triband shunt-fed omnidirectional planar dipole array," *IEEE Antennas Wireless Propag. Lett.*, vol. 9, pp. 850-853, 2010.
- [10] T. J. Judasz and B. B. Balseley, "Improved theoretical and experimental models for the coaxial colinear antenna," *IEEE Trans. Antennas Propag.*, vol. 37, no. 3, pp. 289-296, Mar. 1989.
- [11] H. Miyashita, H. Ohmine, K. Nishizawa, S. Makino, and S. Urasaki, "Electromagnetically coupled coaxial dipole array antenna," *IEEE Trans. Antennas Propag.*, vol. 47, no. 11, pp. 1716-1726, Nov. 1999.
- [12] C.-C. Lin, L.-C. Kuo, and H.-R. Chuang, "A horizontally polarized omnidirectional printed antenna for WLAN application," *IEEE Trans. Antennas Propag.*, vol. 54, no. 11, pp. 3551-3556, Nov. 2006.
- [13] Y. Yu, F. Jolani, and Z. Chen, "A wideband omnidirectional horizontally polarized antenna for 4G LTE application," *IEEE Antennas Wireless Propag. Lett.*, vol. 12, pp. 686-689, 2013.
- [14] C. H. Ahn, S. W. Oh, and K. Chang, "Adual-frequency omnidirectional antenna for polarization diversity of MIMO and wireless communication application," *IEEE Antennas Wireless Propag. Lett.*, vol. 8, pp. 966-970, 2009.
- [15] H.-R. Chuang and L.-C. Kuo, "3-D FDTD design analysis of a 2.4-GHz polarization-diversity printed dipole antenna with integrated balun and polarization-switching circuit for WLAN and wireless communication application," *IEEE Trans. Microw. Theory Techn.*, vol. 51, no. 2, pp. 374-381, Feb. 2003.
- [16] E. Bjornson, L. Van der Perre, S. Buzzi and E. G. Larsson, "Massive MIMO in Sub-6 GHz and mmWave: Physical, Practical, and Use-Case Differences," *IEEE Wirel. Commun.*, vol. 26, no. 2, pp. 100-108, April 2019.
- [17] Abdullah, Qazwan, et al. "Maximising system throughput in wireless powered sub-6 GHz and millimetre-wave 5G heterogeneous networks." *TELKOMNIKA*, 18.3 (2020): 1185-1194.

- [18] F. Linsalata et al., "LoS-Map Construction for Proactive Relay of Opportunity Selection in 6G V2X Systems," *IEEE Trans. Veh. Technol.*, vol. 72, no. 3, pp. 3864-3878, March 2023.
- [19] S. Wu, J. Xu and Q. Chen, "High directivity Omnidirectional Horizontally Polarized Dipole Array for Sub-6 Base Station," *IEEE Antennas Wireless Propag. Lett.*
- [20] S. Xia, C. Ge, Q. Chen and F. Adachi, "A Study on User-antenna Cluster Formation for Cluster-wise MU-MIMO," *2020 23rd International Symposium on Wireless Personal Multimedia Communications (WPMC)*, Okayama, Japan, 2020, pp. 1-6.
- [21] K. Samdanis, X. Costa-Perez and V. Sciancalepore, "From network sharing to multi-tenancy: The 5G network slice broker," *IEEE Commun Mag.*, vol. 54, no. 7, pp. 32-39, July 2016.
- [22] W. Lin and R. W. Ziolkowski, "High-Directivity, Compact, Omnidirectional Horizontally Polarized Antenna Array," *IEEE Trans. Antennas Propag.*, vol. 68, no. 8, pp. 6049-6058, Aug. 2020.
- [23] Z. Liang, L. Huang, W. Xu, Y. Peng, J. Wang and H. Zhang, "Compact High directivity Omnidirectional Horizontally Polarized Antenna Array Utilizing an Aperture With Uniform Field Distribution," *IEEE Trans. Antennas Propag.*, vol. 70, no. 11, pp. 11138-11142, Nov. 2022.
- [24] K. Wei, Z. Zhang, Z. Feng and M. F. Iskander, "A MNG-TL Loop Antenna Array With Horizontally Polarized Omnidirectional Patterns," *IEEE Trans. Antennas Propag.*, vol. 60, no. 6, pp. 2702-2710, June 2012.
- [25] W. Lin and R. W. Ziolkowski, "Compact, High Directivity, Omnidirectional Circularly Polarized Antenna Array," *IEEE Trans. Antennas Propag.*, vol. 67, no. 7, pp. 4537-4547, July 2019.
- [26] P. V. Brennan, A. Narayanan, and R. Benjamin, "Grating lobe control in randomised, sparsely populated MIMO radar arrays," *IET Radar Sonar Navig.*, vol. 6, no. 7, pp. 587 - 594, Aug. 2012.
- [27] W. Roberts, L. Xu, J. Li and P. Stoica, "Sparse Antenna Array Design for MIMO Active Sensing application," *IEEE Trans. Antennas Propag.*, vol. 59, no. 3, pp. 846-858, March 2011.
- [28] D. Jackson and N. Alexopoulos, "directivity enhancement methods for printed circuit antennas," *IEEE Trans. Antennas Propag.*, vol. 33, no. 9, pp. 976-987, September 1985.
- [29] Z. -K. Pan, W. -X. Lin and Q. -X. Chu, "Compact Wide-Beam Circularly-Polarized Microstrip Antenna With a Parasitic Ring for CNSS application," *IEEE Trans. Antennas Propag.*, vol. 62, no. 5, pp. 2847-2850, May 2014.
- [30] I. Gupta and A. Ksienski, "Effect of mutual coupling on the performance of adaptive arrays," *IEEE Trans. Antennas Propag.*, vol. 31, no. 5, pp. 785-791, September 1983.
- [31] J. W. Wallace and M. A. Jensen, "Mutual coupling in MIMO wireless systems: a rigorous network theory analysis," *IEEE Trans. Wirel. Commun.*, vol. 3, no. 4, pp. 1317-1325, July 2004.
- [32] C. -Y. Chiu, C. -H. Cheng, R. D. Murch and C. R. Rowell, "Reduction of Mutual Coupling Between Closely-Packed Antenna Elements," *IEEE Trans. Antennas Propag.*, vol. 55, no. 6, pp. 1732-1738, June 2007.
- [33] R. G. Vaughan and J. B. Andersen, "Antenna diversity in mobile communications," *IEEE Trans. Veh. Technol.*, vol. 36, no. 4, pp. 149-172, Nov. 1987.
- [34] M. S. Siukola, "The Traveling-Wave VHF Television Transmitting Antenna," *IRE Trans. Broadcast Telev. Receiv.*, vol. BTR-3, no. 2, pp. 49-58, Oct. 1957.
- [35] H. R. D. Filgueiras, I. F. da Costa, A. Cerqueira S., J. R. Kelly and P. Xiao, "A Novel Approach for Designing Omnidirectional Slotted-Waveguide Antenna Arrays," *2018 International Conference on Electromagnetics in Advanced Applications (ICEAA)*, Cartagena, Colombia, 2018, pp. 64-67.



JUNYI XU received the bachelor's degree in electronic engineering from the Beijing Institute of Technology University, Beijing, China, in 2017, and the master's degree in electronic engineering from Tohoku University, Sendai, Japan, in 2020, where he is currently pursuing the Ph.D. degree. His research interests include B5G omnidirectional base station antenna design and antenna characteristics in lossy medium.

2016 to 2018, the Chair of IEEE Antennas and Propagation Society Tokyo Chapter from 2017 to 2018. He is now the Chair of IEICE Technical Committee on Antennas and Propagation, IEICE Fellow.



SIRAO WU received the master's degree in from Xidian University, Xi'an, China, in 2017, and the Ph. D from Tohoku University, Sendai, Japan, in 2023. Her research interests include dual-band high gain antennas and B5G omnidirectional broadband base station antennas.



QIANG CHEN received the bachelor's degree from Xidian University, Xi'an, China, in 1986, and the master's degree and Ph. D from Tohoku University, Sendai, Japan, in 1991 and 1994, respectively. He is currently Chair Professor of Electromagnetic Engineering Laboratory with the Department of Communications Engineering, Faculty of Engineering, Tohoku University. His primary research interests include antennas, microwave and millimeter wave, electromagnetic measurement and computational electromagnetics.

Dr. Chen received the Best Paper Award and Zen-ichi Kiyasu Award in 2009 from the Institute of Electronics, Information and Communication Engineers (IEICE). He served as the Chair of IEICE Technical Committee on Photonics-applied Electromagnetic Measurement from 2012 to 2014, the Chair of IEICE Technical Committee on Wireless Power Transfer from